Proceedings of the ASME 2023
International Mechanical Engineering Congress and Exposition
IMECE2023
October 29-November 2, 2023, New Orleans, Louisiana

IMECE2023-112726

SELF-SENSING PIEZOELECTRIC COMPOSITE STRUCTURES VIA GENERATION AND RECEPTION OF ULTRASONIC GUIDED WAVES

Shulong Zhou
University of Michigan-Shanghai Jiao Tong University Joint Institute, Shanghai Jiao Tong University, Shanghai, China

Yanfeng Shen
University of Michigan-Shanghai Jiao Tong University Joint Institute, Shanghai Jiao Tong University, Shanghai, China

ABSTRACT

This paper proposes a novel family of intelligent piezoelectric composite structures for the purpose of establishing structural self-awareness via integrating the function of load bearing with the capability of transmitting and receiving high frequency mechanical waves. To develop a deep insight into the mechanism of the intelligent structure, coupled-field Finite Element Models (FEM) are constructed to conduct the transient dynamic analysis for understanding the wave propagation characteristics in piezoelectric composite beams. In particular, the model employs the Equivalent Average Parameter (EAP) method, utilizing overall and nominal quantities, in order to simulate the self-sensing composites. The guided wave generation and tuning characteristics are investigated utilizing the harmonic analysis model with absorbing boundary conditions. Furthermore, meticulously crafted through a continuous process of material ratio optimization and process step refinement, sample piezoelectric composite plates are fabricated to ensure the highest degree of sensitivity and reliability during experimental demonstration. A pitch-catch active sensing setup is utilized to verify the capability of the piezoelectric composites for generating and receiving ultrasonic guided wave. Moreover, a Scanning Laser Doppler Vibrometer (SLDV) is applied to visualize the waves generated in the structure for analyzing the propagation modes of ultrasonic guided waves in the piezoelectric composite material. The numerical simulations and experimental demonstrations showcase that the proposed piezoelectric composite system possesses great potential for realizing self-awareness for future intelligent structures. The paper finished with summary, concluding remarks, and suggestions for future work.

Keywords: piezoelectricity; composites; structural health monitoring; wave propagation, self-awareness

1. INTRODUCTION

Structural health monitoring (SHM) aims at developing interrogation strategies for evaluating structural integrity and mitigating structural damage risks [1, 2]. The advent of intelligent structures endowed with self-sensing capabilities represents a promising breakthrough in the field of structural engineering. These structures have the potential to remarkably reduce maintenance expenses and forestall catastrophic malfunctions, rendering them an invaluable asset in the current climate of burgeoning demand for safer and more efficient infrastructures. Consequently, the imperative to establish sound SHM practices has grown in significance, and the integration of self-sensing technologies into load-bearing structures has the potential to profoundly augment this crucial aspect of infrastructure management [3].

Piezoelectric materials exhibit both inverse and direct piezoelectric properties, enabling them to function as actuation and sensing elements. The piezoelectric wafer active sensor (PWAS) is a notable instance of such materials that has found extensive utilization as a vital component in the generation and reception of ultrasonic guided waves [2-7]. The installation of sensors remains an essential requirement. However, the surface-bonding approach has a weakness in that sensors attached in this way can become debonded and peeled off, and are vulnerable to scratches. Moreover, the physical properties of these sensors are characterized by both brittleness and stiffness, largely dependent on the materials exploited and the processing conditions involved.

On the other hand, the consensus among researchers that embedding sensors into structures is crucial for achieving structural self-awareness. Minakuchi and Takeda employed a new technique utilized fiber optic sensors to detect impact damage in aerospace composite structures, introducing the concepts of "smart crack arrester" and "hierarchical sensing system" [8]. Krishnamurthy et al. achieved delamination

detection via embedding layers of magnetostrictive particles in composite laminates [9]. Paget et al. conducted experiments on the performance of embedded piezoceramic transducers in mechanically loaded composites, revealing a low survival rate of the sensors [10]. However, such embedding approaches of this nature may result in stress concentration within the materials, ultimately leading to the incubation of local cracks.

In an alternative approach, researchers have attempted to manipulate material properties for incorporating functional components. Tallman and his colleagues utilized carbon nanofiber/polyurethane composites forming nanocomposites, resulting in better delamination detection and distributed strain sensing [11]. Gallo and Thostenson incorporated carbon nanotubes into composites to create self-sensing structures capable of monitoring micro cracks [12]. Haghiashtiani and Greminger explored polyvinylidene fluoride (PVDF) as the composite matrix for integrating structural load sensing [13]. Liu et al. fabricated PVDF-TrFE transducers to measure defects in multilayer bonded structures using the ZGV waves [14]. Li et al. developed a coated sensor network made of carbon nanotubes (CNTs) to spray and be deposited onto the surface of the complex structures [15]. The new technique eliminates potential drawbacks associated with the distributed sensors. Certainly, these pioneering approaches have shown drawbacks in terms of low actuation capability and increased costs. Therefore, the development of a novel structure-sensor integration system is essential to usher in a new era of self-sensing smart structures.

This paper presents an intelligent piezoelectric composite beam designed to attain structural self-awareness through the integration of load-bearing function and high-frequency mechanical wave transmission and reception capabilities. Coupled-field Finite Element Models (FEM) are constructed and utilized for comprehending wave propagation features in piezoelectric composite beams. Finally, a pitch-catch active sensing setup is experimentally constructed to verify the piezoelectric composites' ability to generate and receive ultrasonic guided wave signals. Additionally, a Scanning Laser Doppler Vibrometer (SLDV) is employed to visualize the waves generated and propagating in the piezoelectric composite beam.

2. NUMERICAL MODELING OF PIEZOELECTRIC COMPOSITES FOR ESTABLISHING STRUCTURAL SELF-AWARENESS

In this section, the finite element model (FEM) of the proposed piezoelectric composite structure is presented, with its fundamental parameters. Subsequently, delving into an exploration of intrinsic tuning characteristics of the piezoelectric composite beam to investigate the generation and reception characteristics for the ultrasonic wave active sensing.

2.1 Parameterization of the piezoelectric composite

FIGURE 1 illustrates the schematic model of the piezoelectric composite structure, portrayed as a rectangular excavation from the piezoelectric composite material. The preparation techniques involve amalgamating the piezoelectric ceramic (PZT) powder with resin adhesive in a precise proportion, and subsequently, casting it into the mold. The glass fiber was laid evenly and orderly in the structure as glass fiber sheets, whereas the electrode's formation is conducted via coating the surface of the structure with silver. The attainment of actuation and sensing capabilities is facilitated through the curing, vacuuming, and polarization processes, while the incorporation of glass fiber material takes the responsibility of enhancing the tensile strength and design flexibility.

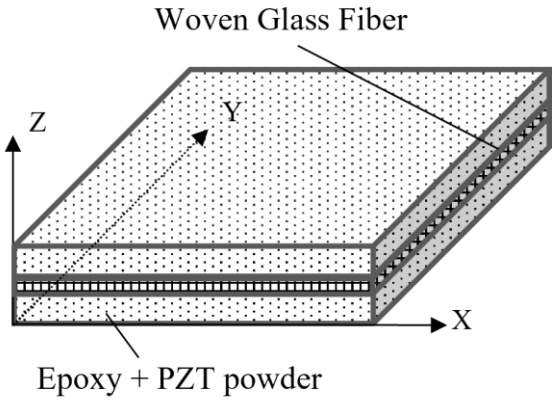

FIGURE 1: SCHEMATIC OF THE PIEZOELECTRIC COMPOSITE STRUCTURAL LAMINA

The FEM expounded in this paper utilized the Equivalent Average Parameter (EAP) method, whereby a complete plate with several layers of lamina was assumed to be a homogeneous entity. The determination of the stiffness matrix of the piezoelectric composite is achieved through scaling an equivalent PZT material stiffness matrix in proportion to the modulus of elasticity of the glass fiber, thereby attaining an equivalent effect:

$$\left[C_p\right] = \begin{bmatrix} 21 & 10.61 & 10.61 & 0 & 0 & 0 \\ 10.61 & 21 & 10.61 & 0 & 0 & 0 \\ 10.61 & 10.61 & 18.18 & 0 & 0 & 0 \\ 0 & 0 & 0 & 5.195 & 0 & 0 \\ 0 & 0 & 0 & 0 & 4.76 & 0 \\ 0 & 0 & 0 & 0 & 0 & 4.76 \end{bmatrix} \text{GPa} \quad (1)$$

As opposed to the existing PZT, the piezoelectric composite material manifests a decrease in the piezoelectric coefficient, owing to the scattered arrangement of powder particles. The present paper posits the definition of the piezoelectric matrix as being equivalent to one-half of the PZT4 piezoelectric matrix:

$$[e_p] = \begin{bmatrix} 0 & 0 & -4.01 \\ 0 & 0 & -4.01 \\ 0 & 0 & 9.16 \\ 0 & 0 & 0 \\ 0 & 6.42 & 0 \\ 6.42 & 0 & 0 \end{bmatrix} \text{C/m}^2 \quad (2)$$

Assuming a density of 1960 kg/m^3 for the piezoelectric composite material, it is additionally hypothesized that the dielectric matrix satisfies identical specifications to the PZT materials:

$$[\varepsilon_p] = \begin{bmatrix} 4.3 & 0 & 0 \\ 0 & 4.3 & 0 \\ 0 & 0 & 4.3 \end{bmatrix} \quad (3)$$

2.2 Mode tuning effects of the piezoelectric composite

To ascertain the characteristics of guided wave generation, the conventional methodology necessitates conducting tuning experiments utilizing the pitch-catch technique to capture signal from transducers. In particular, PWASs are affixed onto the surfaces of host structures, and the amplitudes of multimodal guided waves are recorded across a spectrum of frequencies [16]. The determination of the excitability of each distinct wave mode arises as a consequential facet of this research. In light of the objectives of this research endeavor, the FEM was harnessed to acquire a comprehensive understanding of the generation characteristics of diverse wave modes in piezoelectric composite plates. Mode tuning models with absorbing boundary conditions were constructed as depicted in FIGURE 2a. To eliminate reflections, non-reflective boundaries (NRBs) were used surrounding the piezoelectric composite plate. Within the model, the excitation electrode (6 mm in diameter) was denoted by a green circular area situated upon both upper and lower surfaces of the plate, then coupled to enact the application of the excitation voltage. The bottom electrode potential was set to 0, simulating the grounding condition. Red dots on the plate indicated the sensing points where displacement information was recorded during harmonic analysis. To ensure computational accuracy, caution was paid in dealing with frequency extrema at both the low and high ends of the frequency range. The numerical model required the efficient absorption of all waves by the NRB, which meant that the length of the NRB region should be greater than twice the maximum wavelength of the guided wave mode under consideration. The longest wavelength was observed at the low extrema of the frequency range, which was the S0 mode at 200 mm at 20 kHz. Therefore, the NRB region was set to 400 mm. Conversely, at the high extrema of the frequency range, the shortest wavelength has to be carefully considered as well. In order to accurately predict the wave motion, the mesh size had to be smaller than 1/20th of the smallest wavelength scale. The element size was set to 0.2 mm to ensure that the mesh size was smaller than 1/20th of the shortest wavelength up to 500 kHz, occurred at the A0 mode with a value of 4 mm. This ensures that the guided wave generation characteristics in the frequency range of 20 kHz to 500 kHz enable to be accurately predicted by the FEM.

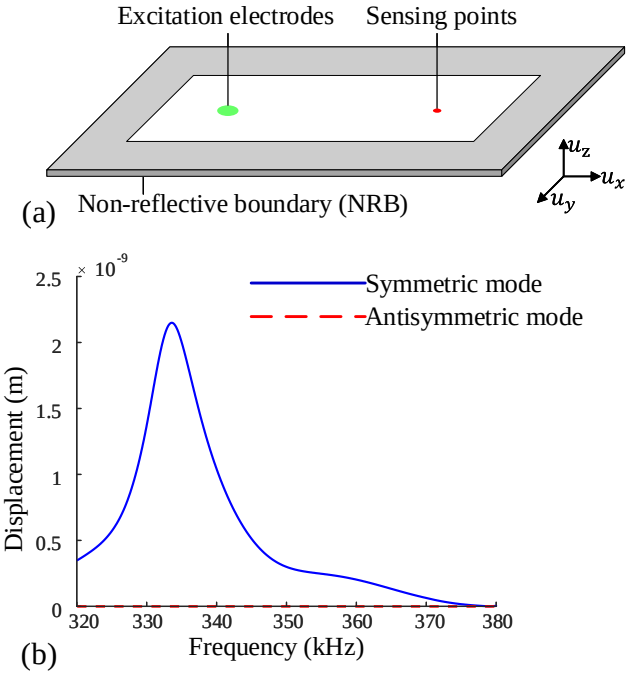

FIGURE 2: (A) THE TUNING FE MODEL; (B) GUIDED WAVE TUNING CHARACTERISTICS IN A 2-MM THICK PIEZOELECTRIC COMPOSITE PLATE

FIGURE 2b presents the variation of horizontal displacement amplitude with frequency for the S0 and A0 modes in a 2-mm thick piezoelectric composite plate from 320 kHz to 380 kHz. The wave generation amplitude of the S0 mode initially increases, reaching a peak at approximately 335 kHz, before decreasing again. Comparing the conventional PWAS-generated multimodal guided waves that include both S0 and A0 components, only the single S0 wave mode was stimulated here. Therefore, such a characteristic allows piezoelectric composite plates to achieve single mode interrogation and significantly reduce the complexity of sensing signals.

2.3 Simulation of pitch-catch active sensing

FIGURE 3 displays the three-dimensional FEM for modeling wave generation and reception. To scrutinize the characteristics of wave propagation, a piezoelectric composite plate measuring 560 mm in length, 140 mm in width, and 1 mm in thickness was utilized. This plate was endowed with polarization electrodes functioning as a transmitter-receiver pair, situated 420 mm apart from one another. In order to actuate the electrode, a 180kHz 150 Vpp 3-count Hanning window modulated sine tone burst signal was employed. The time step was defined as 0.25 μs, fulfilled the accuracy requisite of the excitation frequency. The NRB was implemented for eliminating the reflection of waves from the edges of the plate.

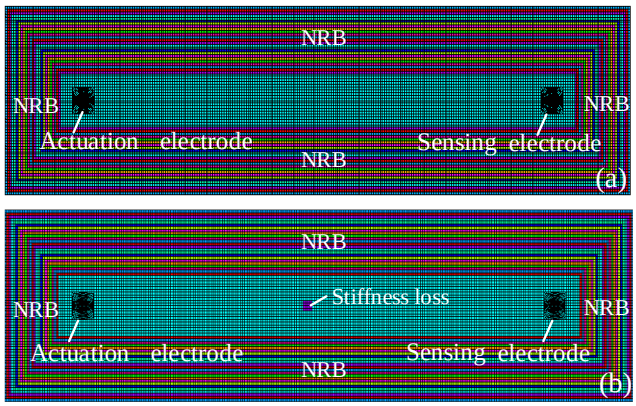

FIGURE 3: FINITE ELEMENT MODEL FOR STUDYING WAVE GENERATION AND RECEPTION IN THE PIEZOELECTRIC COMPOSITE A) PRISTINE CASE; B) DAMAGED CASE

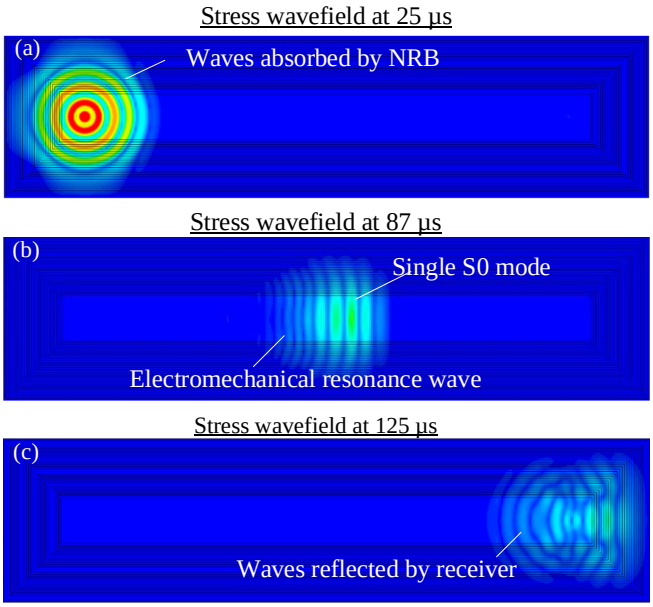

FIGURE 4: SNAPSHOTS OF STRESS WAVEFIELD IN PRISTINE CASE AT A) 25 MS; B) 65 MS; C) 125 MS

FIGURE 4 presents a depiction of the stress wavefield at distinct time intervals, whereby only a solitary S0 wave mode was observed. The guided waves generated by the actuation electrode were instantaneously detected at the sensing location as a direct incident wave packet. This discovery represented a significant departure from the customary PWAS-generated multimodal guided waves, typically encompassed both S0 and A0 components. Additionally, the non-reflective boundaries were observed to be effective in absorbing the incident waves. Subtle sequential waves, stemming from the resonating coupling effect at the piezo electrode, were also noticed. Once the guided wave propagated to the receiving electrode, then the mechanical wave instantaneously interacted with it. The distinctive feature forms the key directions of to the design of subsequent sensing neurons on such a smart structure.

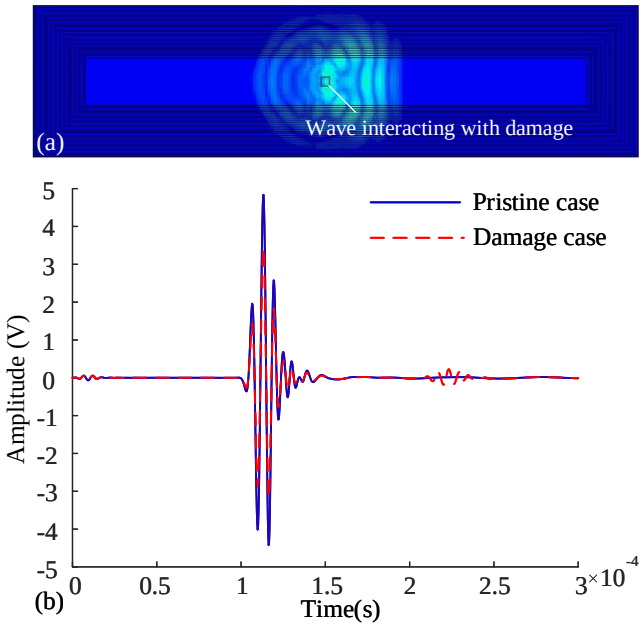

FIGURE 5: A) SNAPSHOT OF STRESS WAVEFIELD IN DAMAGE CASE; B) ACTIVE SENSING SIGNALS OF THE PRISTINE AND DAMAGED CASE

The stress wavefield in the damaged case is depicted in FIGURE 5a, wherein the simulation involved a reduction in the local material stiffness dispersing at a small region to simulate structural damage. Scattered waves emanating from the damaged site was readily identified in FIGURE 5b. The discernible decline in the apparent amplitude between the pristine and damaged case is evident, presenting a viable option for characterizing the damage. The signal originating from the damage reflection was of particular interest, as it triggered the emergence of a wavelet packet at the conclusion of the received signal. This remarkable phenomenon presents promising opportunities for damage characterization, paving the way towards the current research goal.

3. FABRICATION OF PIEZOELECTRIC COMPOSITE TEST SPECIMEN

The customized piezoelectric composite structure was characterized by the absence of intricate assembly processes, without involving sintering under high-temperature environments during fabrication compared with piezoelectric ceramics. Hence, to attain optimal piezoelectric properties of the specimens, the formulation of the process flow and production links requires further exploration. Accordingly, the polarized voltage, particle size of the powder, and mesh size of the glass fiber are investigated to achieve the desired piezoelectric properties.

TABLE 1,2, and 3 showcase the measurement parameters about diverse cases. The analysis of these three studies revealed that the dielectric loss was significantly higher compared to the conventional piezoelectric ceramics. Additionally, the piezoelectric strain constant exhibited an increase with the rise

in polarization voltage. However, it was observed that an increase in the particle size of the piezoelectric ceramic powder led to a larger piezoelectric strain constant. This was attributable to the fact that the resin glue constituted the bulk of the material, and there was a limited amount of piezoelectric ceramic powder per unit volume, resulting in a significant reduction in the piezoelectric effect. The piezoelectric properties were not directly correlated with the mesh thickness of the glass fiber. Finally, based on the findings, the optimal parameters included a particle size of piezoelectric ceramic powder of 0.125 mm, a polarization voltage of 9 kV/mm, and a glass fiber grid size of 10 mm.

TABLE 1: THE MEASUREMENT PARAMETERS OF THE SPECIMEN UNDER DIVERSE POLARIZED VOLTAGE

	Capacitance C (pF)	Dielectric loss Tgδ (%)	Piezoelectric strain constant d33 (pC/N)
9kV/mm	12	2.72	31
6kV/mm	18	3.521	26
3kV/mm	17	2.355	25

TABLE 2: THE MEASUREMENT PARAMETERS OF THE SPECIMEN UNDER DIVERSE PARTICLES SIZES

	Capacitance C (pF)	Dielectric loss Tgδ (%)	Piezoelectric strain constant d33 (pC/N)
0.048mm	21	2.558	33
0.075mm	27	3.12	38
0.125mm	27	4.561	44

TABLE 3: THE MEASUREMENT PARAMETERS OF THE SPECIMEN UNDER DIVERSE MESH SIZES OF GLASS FIBER

	Capacitance C (pF)	Dielectric loss Tgδ (%)	Piezoelectric strain constant d33 (pC/N)
10mm	28	4.324	23
12mm	27	3.327	22
14mm	27	4.271	23
16mm	29	5.589	22

The fabrication process of the piezoelectric composite structure involved the blending of PZT powder and epoxy resin at a weight ratio of 5:1. The epoxy resin comprised resin (HF-005) and hardener (HF-006), was procured from Wuxi City Huifeng Electronic Co., Ltd. A meticulous preparation approach was employed, wherein the blended mixture underwent ultrasonication for dispersion through vacuum-based equipment. Subsequently, the mixture was carefully poured into a designated mold which has been laid the glass fiber layer and subjected to a vacuum device to eliminate any bubbles during the curing process. The curing process was carried out at a constant temperature of 60 degrees Celsius for a duration of 4 hours. To achieve a polarized piezoelectric composite structure, the poling electrodes were coated with silver screen printing at an elevated temperature of 110 degrees Celsius for a period of 45 minutes. Poling was executed utilizing a high-voltage amplifier submerged in oil, with a voltage of 6 kV for a duration of 15 minutes. To ensure complete polarization, special attention was given to the initial polarization electrode's coverage of the entire upper and lower surface of the piezoelectric composite structure. The specimen was machined to meet precise dimensional requirements, and the excess silver layer was removed from the surface of the structure through laser carving, retaining the necessary electrode parts. FIGURE 6 illustrates the manufacturing process of the piezoelectric composite structure, demonstrating the meticulous approach employed to fabricate a highly polarized, precisely dimensioned piezoelectric composite beam.

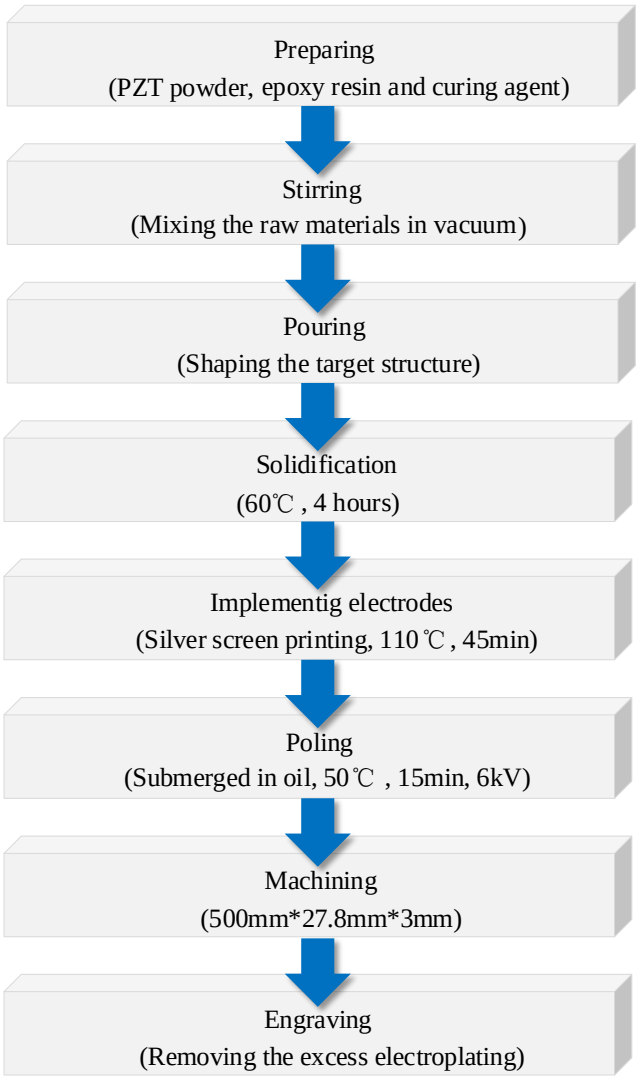

FIGURE 6: FLOW CHART OF MANUFACTURING PROCEDURE FOR THE PIEZOELECTRIC COMPOSITE STRUCTURE

FIGURE 7 presents the beam specimen fabricated by the piezoelectric composite. The upper and lower surfaces of the beam were strategically fitted with nine pairs of electrodes

measuring 10 mm in diameter, positioned with a distance of 50 mm between each pair, to facilitate subsequent electrode voltage loading. Significantly, to ensure optimal electrode voltage loading, a portion of the silver layer was intentionally preserved, serving as a conductive connector. The utilization of these connectors established the reliability of the interface, facilitating the use of a gentle and convenient connection, so as to prevent any unforeseen damage or failure, consequently enhancing its resilience and practicality.

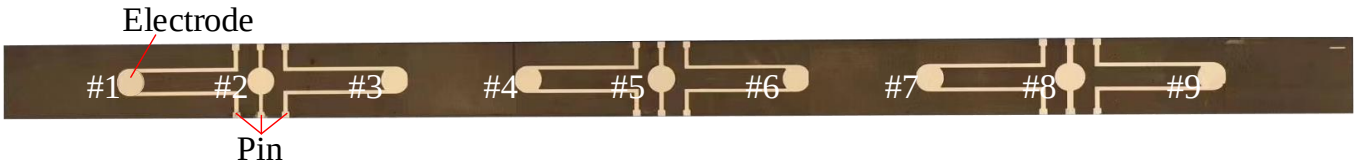

FIGURE 7: PIEZOELECTRIC COMPOSITE BEAM SPECIMEN FOR EXPERIENTAL TESTS

4. EXPERIMENTAL DEMONSTRATION OF SELF-AWRENESS OF PIEZOELECTRIC COMPOSITE STRUCTURES

Experimental demonstration is delivered in this section to substantiate the guided wave transmission and reception capability of the piezoelectric composite structure. Finally, guided-wave propagation phenomena are presented through the wavefield visualization utilizing the SLDV measurements.

4.1 Experimental demonstration of the guided wave transmission and reception

In order to demonstrate the tuning effect and self-sensing capability of the piezoelectric composite beam, a pitch-catch experimental setup is designed in FIGURE 8. A Keysight 33500B arbitrary function generator was used to generate excitation waveforms of 3-count Hanning window modulated sine tone bursts. The excitation signal was further amplified to 175 Vpp by a Krohn-hite 7602 M wideband power amplifier and was applied on the actuation electrodes. At each end of the specimen, sponge blocks were positioned while the crocodile clamp was attached at the designated connectors to establish a detachable connection.

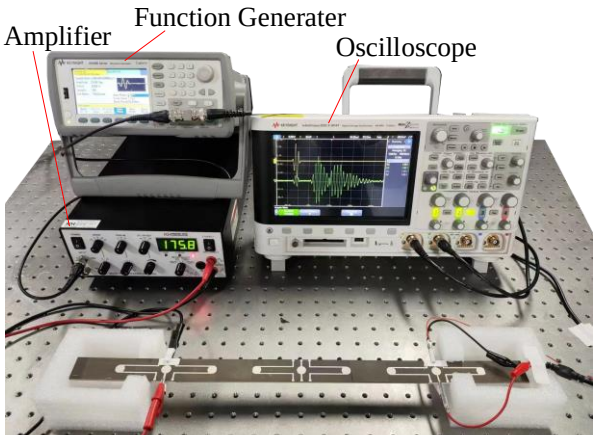

FIGURE 8: EXPERIMENTAL SETUP FOR GUIDED WAVE CHARACTERIZATION OF A PIZOELECTRIC COMPOSITE BEAM

A methodical sequence of experiments was undertaken on the piezoelectric composite beam to procure the sensing signal for tuning analysis, consistent with the numerical predictions. As expounded upon in the simulation, the piezoelectric composite beam illustrated lacks any antisymmetric wave in FIGURE 9. The tuning characteristic derived from the experiment exhibited disparities from the numerical results owing to the higher overall damping of the material in the manufactured specimen. The global tunning peak underwent a shift towards lower frequencies and gradually decreased in the high frequency range, primarily due to dissipative attenuation. This occurrence offers an effective point of reference for the selection of the excitation frequency in subsequent pitch-catch experiments.

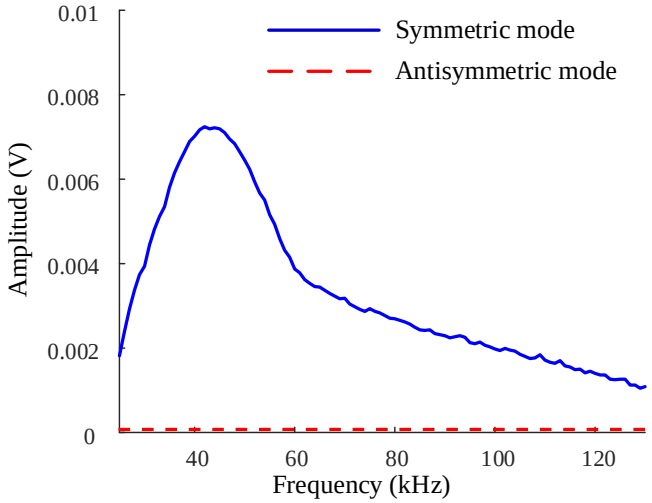

FIGURE 9: GUIDED WAVE TUNING CHARACTERISTICS IN A 2-MM THICK PIEZOELECTRIC COMPOSITE BEAM

FIGURE 10c presents the active sensing signals of the pristine and damaged case. To assess the local structural impairment, an iron block was affixed onto the surface of the specimen for mimicking a structural damage in FIGURE 10b. The resultant signal responses displayed a noticeable reduction in amplitude and greater intricacy compared to the numerical results. This phenomenon was attributed to the combined superposition of wave packets, wherein the reflected

symmetrical waves from beam boundaries were overlapped with the incident symmetrical waves.

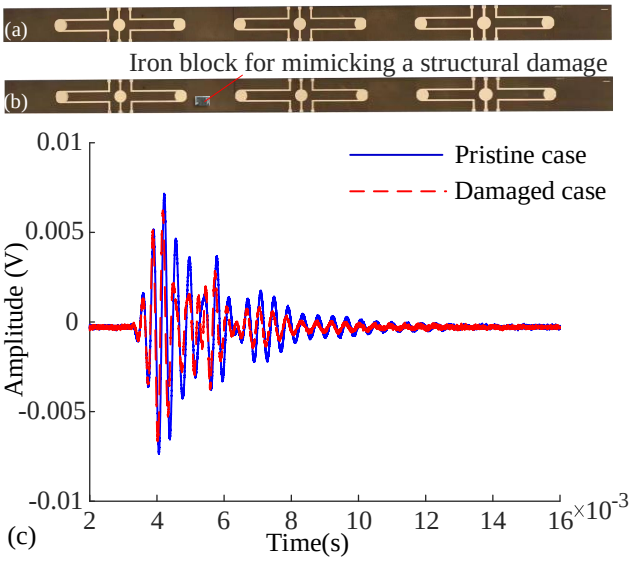

FIGURE 10: EXPERIMENTAL DETAILS: A) PRISTINE CASE; B) DAMAGED CASE; C) EXPERIMENTAL ACTIVE SENSING SIGNALS OF THE PRISTINE AND DAMAGED CASE

4.2 Experimental visualization of the wavefield

To further verify the active sensing capability of the functional composite, SLDV experiments were performed to visually capture the wavefield propagation within the piezoelectric composite beam in FIGURE 11a and FIGURE 12a. For demonstrating the exclusive production of S-mode waves without any accompanying A-mode waves, the beam specimen underwent testing on two separate occasions. In the first round, the laser head pointed perpendicularly towards the beam surface to record the out-of-plane velocity component in FIGURE 11b. In the second round, the specimen was tilted to introduce an inclination angle between the laser ray and the upper surface of the beam, as shown in FIGURE 12b. Damping clay was wrapped on both ends the beam to absorb the boundary reflections. The laser scanning area was coated by the reflective tape to enhance the intensity of planar surface reflection. The experimental test involved the generation of a 3-count Hanning window modulated sine tone burst by the Keysight 33500B arbitrary function generator. The excitation waveform was subsequently amplified to 190 Vpp by the Krohn-hite 7602 M wideband power amplifier and applied to the actuation electrode.

Temporal-domain snapshots of the propagating wavefields are depicted in FIGURE 11c and FIGURE 12c. Guided waves were generated and propagated towards the sensing elements. The resultant wavefield in the piezoelectric composite beam region was subsequently captured by the SLDV, processed employing the Polytec system, and presented as visualized wavefield images. Notably, when the specimen was tilted, the induced vibration was not solely a vertical out-of-plane displacement in the beam, but rather a superposition of in-plane and out-of-plane displacements. The purely out-of-plane displacement was nearly negligible, demonstrating the dominating component as symmetric wave modes. These observations unequivocally corroborate the theoretical analysis findings.

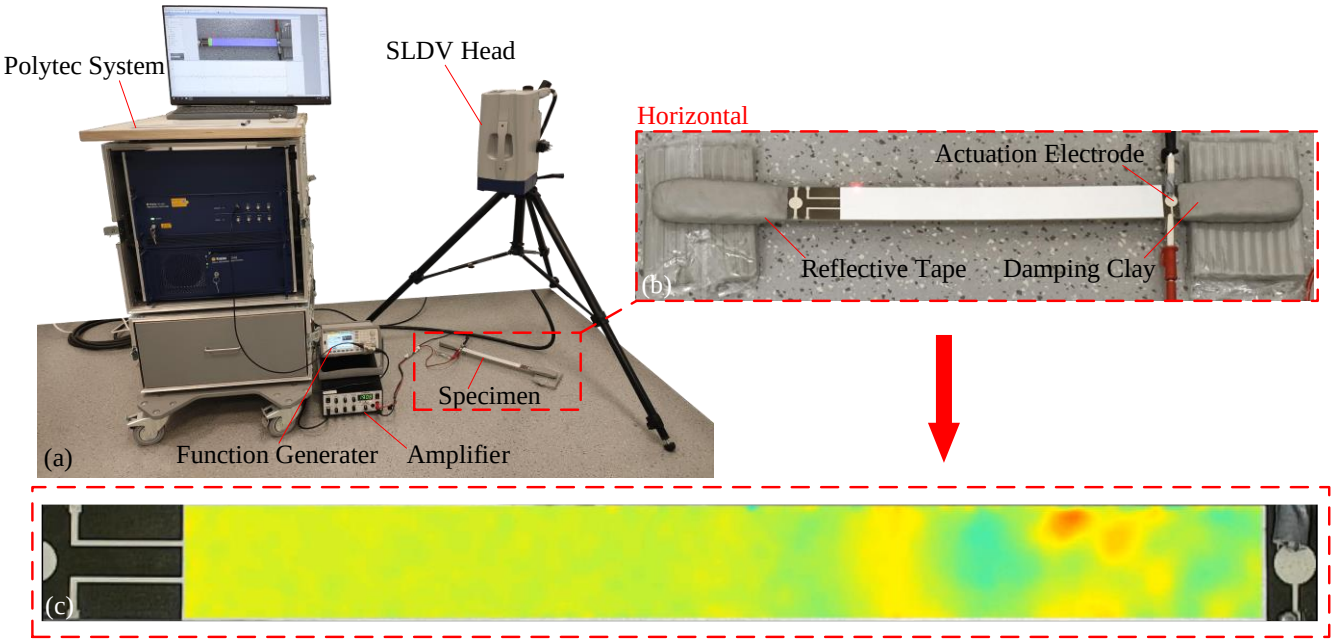

FIGURE 11: A) EXPERIMENTAL SETUP USING 1D-SLDV FOR WAVEFIELD VISUALIZATION; B) EXPERIMENTAL SPECIMEN FOR SLDV TESTS AND ZOOM-IN DETAILS OF HORIZONTAL DISPLACEMENT; C) TEMPORAL-DOMAIN SNAPSHOTS OF THE PROPAGATING WAVEFIELDS

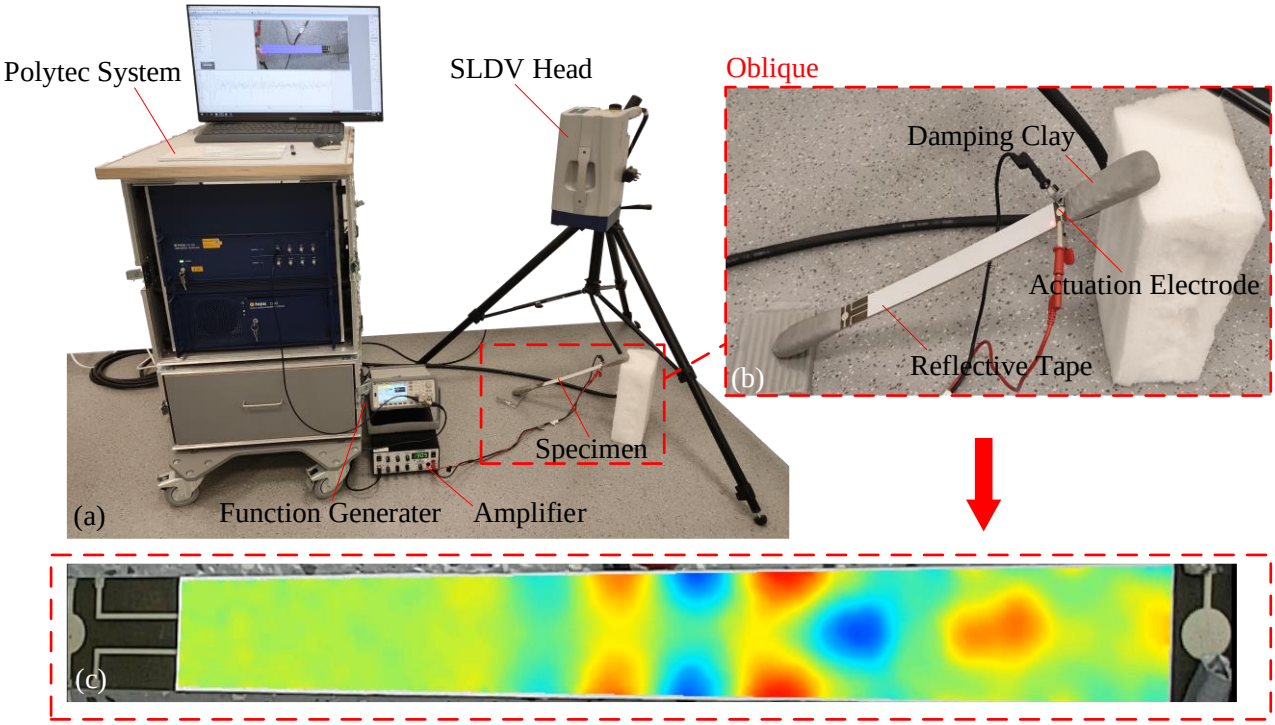

FIGURE 12: A) EXPERIMENTAL SETUP USING 1D-SLDV FOR MEASURING; B) EXPERIMENTAL SPECIMEN FOR SLDV TESTS AND ZOOM-IN DETAILS OF OBLIQUE DISPLACEMENT; C) TEMPORAL-DOMAIN SNAPSHOTS OF THE PROPAGATING WAVEFIELDS

5. RESULTS, DISCUSSION AND CONCLUSION

This paper presented an intelligent piezoelectric composite beam that combines load-bearing functionality with the capacity to transmit and receive high-frequency mechanical waves. The study employed a coupled-field FEM to systematically analyze the wave propagation features in piezoelectric composite beams, and experimentally validated the guided wave transmission and reception capabilities via a pitch-catch active sensing setup. The waves generated in the beam were visualized using the SLDV. It was found that a single symmetric wave mode was generated and propagated as the interrogative field. An obvious tuning phenomenon was also demonstrated. The active material beam showed its outstanding performance for detecting damage sites in the structure.

In the future, further investigations would be conducted to explore the optimization of the composite beam design and material properties to enhance its performance in detecting damage sites in structures. Additionally, the utilization of advanced signal processing techniques and machine learning algorithms could be able to explored to improve the accuracy and efficiency of damage detection and localization. This could involve developing intelligent algorithms extracting valuable information from the wave signals and provide real-time monitoring and analysis of structural health. In summary, the proposed piezoelectric composite possesses superb potential to establish structural self-awareness through active sensing schemes, paving the way towards the further advancement of smart structures.

ACKNOWLEDGEMENTS

The support from the National Natural Science Foundation of China (contract numbers 51975357 and 51605284) and the Shanghai Rising-Star Program (contract number 21QA1405100) are thankfully acknowledged. This work was also sponsored by the Wuxi City Huifeng Electronic Co., Limited.

REFERENCES

[1] Y. Shen, J. Wang, and W. Xu, “Nonlinear features of guided wave scattering from rivet hole nucleated fatigue cracks considering the rough contact surface condition,” *Smart Mater. Struct.*, vol. 27, no. 10, p. 105044, Oct. 2018, doi: 10.1088/1361-665X/aadd2d.

[2] J. Wang, Y. Shen, D. Rao, and W. Xu, “Physical-virtual time reversing of nonlinear Lamb waves for fatigue crack detection and quantification,” *Mech. Syst. Signal Process.*, vol. 160, p. 107921, Nov. 2021, doi: 10.1016/j.ymssp.2021.107921.

[3] Jinping Ou and Hui Li, “Structural Health Monitoring in mainland China: Review and Future Trends,” *Struct. Health Monit.*, vol. 9, no. 3, pp. 219–231, May 2010, doi: 10.1177/1475921710365269.

[4] G. Victor, “Structural health monitoring with piezoelectric wafer active sensors – predictive modeling and simulation,” *INCAS Bull.*, vol. 2, no. 3, pp. 31–44, Sep. 2010, doi: 10.13111/2066-8201.2010.2.3.4.

[5] A. Ebrahimkhanlou, B. Dubuc, and S. Salamone, “Damage localization in metallic plate structures using

edge-reflected lamb waves," *Smart Mater. Struct.*, vol. 25, no. 8, p. 085035, Aug. 2016, doi: 10/gp4nqz.

[6] X. Zhao, H. Gao, G. Zhang, B. Ayhan, and F. Yan, "Active health monitoring of an aircraft wing with embedded piezoelectric sensor/actuator network: I. Defect detection, localization and growth monitoring," *Smart Mater. Struct.*, vol. 16, no. 4, pp. 1208–1217, Aug. 2007, doi: 10.1088/0964-1726/16/4/032.

[7] Lingyu Yu and V. Giurgiutiu, "Multi-mode Damage Detection Methods with Piezoelectric Wafer Active Sensors," *J. Intell. Mater. Syst. Struct.*, vol. 20, no. 11, pp. 1329–1341, Jul. 2009, doi: 10.1177/1045389X08096665.

[8] S. Minakuchi and N. Takeda, "Recent advancement in optical fiber sensing for aerospace composite structures," *Photonic Sens.*, vol. 3, no. 4, pp. 345–354, Dec. 2013, doi: 10.1007/s13320-013-0133-4.

[9] A. V. Krishnamurthy, M. Anjanappa, Z. Wang, and X. Chen, "Sensing of Delaminations in Composite Laminates using Embedded Magnetostrictive Particle Layers," *J. Intell. Mater. Syst. Struct.*, vol. 10, no. 10, pp. 825–835, Oct. 1999, doi: 10.1106/6UR5-7LE3-QV3H-AG6V.

[10] C. A. Paget, K. Levin, and C. Delebarre, "Actuation performance of embedded piezoceramic transducer in mechanically loaded composites," *Smart Mater. Struct.*, vol. 11, no. 6, pp. 886–891, Dec. 2002, doi: 10.1088/0964-1726/11/6/309.

[11] T. N. Tallman, S. Gungor, K. W. Wang, and C. E. Bakis, "Tactile imaging and distributed strain sensing in highly flexible carbon nanofiber/polyurethane nanocomposites," *Carbon*, vol. 95, pp. 485–493, Dec. 2015, doi: 10.1016/j.carbon.2015.08.029.

[12] G. J. Gallo and E. T. Thostenson, "Electrical characterization and modeling of carbon nanotube and carbon fiber self-sensing composites for enhanced sensing of microcracks," *Mater. Today Commun.*, vol. 3, pp. 17–26, Jun. 2015, doi: 10.1016/j.mtcomm.2015.01.009.

[13] G. Haghiashtiani and M. A. Greminger, "Fabrication, polarization, and characterization of PVDF matrix composites for integrated structural load sensing," *Smart Mater. Struct.*, vol. 24, no. 4, p. 045038, Apr. 2015, doi: 10.1088/0964-1726/24/4/045038.

[14] Q. Liu, Y. Li, R. Guan, J. Yan, and M. Liu, "Advancing measurement of zero-group-velocity Lamb waves using PVDF-TrFE transducers: first data and application to in situ health monitoring of multilayer bonded structures," *Struct. Health Monit.*, p. 147592172211268, Nov. 2022, doi: 10.1177/14759217221126812.

[15] W. Li, W. Liu, L. M. Zhou, H. Zhang, and Y. Lu, "A COATED CARBON NANOTUBE SENSOR NETWORK FOR IN-SITU ACTIVE SENSING OF ULTRASONIC ELASTIC WAVES," 2015.

[16] G. Santoni, L. Yu, B. Xu, and V. Giurgiutiu, "Lamb Wave-Mode Tuning of Piezoelectric Wafer Active Sensors for Structural Health Monitoring An analytical and experimental investigation of the Lamb wave-mode tuning with piezo," Apr. 2023.